27th EPS Conference on Contr. Fusion and Plasma Phys. Budapest, 12-16 June 2000 ECA Vol. **24B** (2000) 1108 -1111

Active feedback stabilization of nonaxisymmetric modes in tokamaks

A. Bondeson[1], Y. Q. Liu[1], C. M. Fransson[2], B. Lennartson[2], C. Breitholtz[2]

[1]*Department of Electromagnetics, EURATOM-NFR/Fusion Association*
[2]*Department of Signals and Systems, Control and Automation Laboratory*
Chalmers University of Technology, S-412 96 Göteborg, Sweden

1. Introduction

Advanced tokamaks with negative central shear can achieve significantly improved energy confinement. However, to achieve both high bootstrap current fraction and sufficient β, high normalized beta, in excess of the free boundary limit [1, 2] is required, unless the cross section is very elongated or the aspect ratio is very low. Stabilization by nearby, ideally conducting walls can raise the beta limit for external modes. However, with a finitely conducting wall, resistive wall modes (RWM) generally become unstable on the time-scale over which eddy currents in the wall decay. Non-axisymmetric RWM's can be stabilized by rotation, but this requires uncomfortably high rotation velocities. A more promising approach is active feedback. Experiments on feedback stabilization of high-beta RWM are in progress on the DIII-D tokamak [3], and theoretical analyses have been carried out recently [4, 5, 6, 7].

In this paper, we present results on feedback stabilization from toroidal stability calculations. We also discuss controller design and compare the performance and robustness of optimal controllers with different structures [7].

2. Toroidal calculations

We have added sensor and feedback coils to the toroidal MHD stability code MARS [5, 6]. The geometry of the feedback system is shown in Fig. 1. The number of coils in the toroidal direction is assumed large enough so that the feedback current can be described as a single n surface current. We consider one single toroidal array of active and sensor coils, located in the outboard mid-plane.

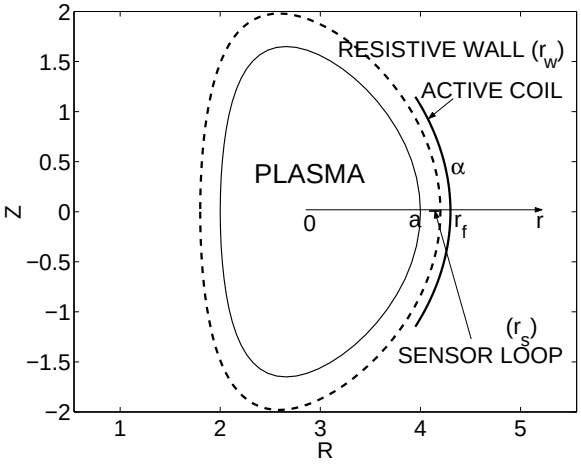

Figure 1: *Geometry of feedback control.*

The minor radii of the active coil, the resistive wall, and the sensor loop are denoted by r_f, r_w, and r_s respectively. The poloidal width of the active coil is measured by $\alpha = \Delta\chi/\pi$ (the fraction of half the circumference, subtended by the active coil). In Fig. 1 the sensor loop detects the *poloidal* component of the magnetic field. We call this scheme b_θ*-sensor* feedback. The MARS code can also simulate b_r*-sensor* feedback, where the sensor loop detects the *radial* component of the magnetic field.

The MARS code can model proportional current control, or a more realistic feedback model, where the controller produces a voltage across the active coil. The transfer function of the plasma-wall system for current control is denoted by $P_1(s)$. In addition, a transfer function $P_2(s)$ is calculated, repre-

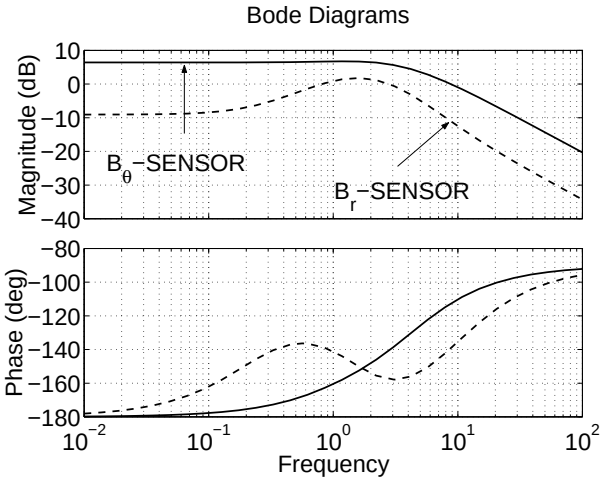

Figure 2: *Bode plots of typical open loop transfer functions $P_1^r(s)$ and $P_1^\theta(s)$ for b_r and b_θ sensors. The same equilibrium and feedback configuration are used as in Fig. 2.*

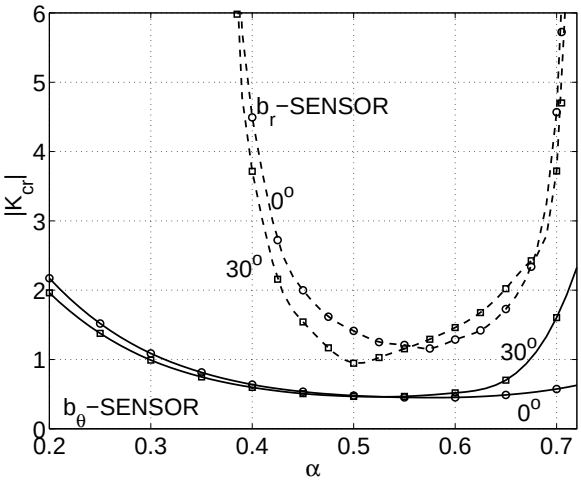

Figure 3: *Magnitude of the critical gain $|K_{\rm cr}|$ versus the active coil width for the b_r-sensor (dashed lines) and b_θ-sensor (solid lines) feedback schemes.*

senting a normalized, "loaded" self-inductance of the feedback coil. Typically, these transfer functions are rather simple and can be approximated by low order rational functions, or Padé approximations, derived from a small number of MARS runs [5]. The resulting process transfer function for voltage control is [6]

$$G(s) = \frac{P_1(s)}{1 + s\tau P_2(s)}, \qquad (1)$$

where τ is the ratio of control system response time to the resistive wall time.

Figure 2 shows the transfer functions $P_1^r(s)$ and $P_1^\theta(s)$ for b_r- and b_θ-sensor feedback respectively. The calculations were made for a JET-like advanced equilibrium with $q_{\rm min} = 1.6, q_a = 3.4$, normalized current $I_N = 1.71$, low inductance $l_i = 0.61$, and normalized beta $\beta_N \simeq 4.7$. The pressure is far above the no-wall limit of $\beta_N \simeq 2.9$, and the marginal position for an ideal wall is $r_w = 1.3a$. We chose to place the resistive wall at $r_w = 1.2a$. We place active coils of width $\alpha = 0.5$ at $r_f = 1.3a$, and small sensor coils in the outboard mid-plane, just inside the wall.

It is easy to understand that the poloidal sensor gives a larger response and smaller phase lag at high frequency, $\omega\tau_w \gg 1$, where the wall acts almost like a perfect conductor. The Bode plot also draws attention to the more important difference between the poloidal and radial sensors at low frequency. This can be understood by noting that at low frequency, the plasma-induced radial field [that *opposes* the feedback field, since $\arg(P_1) \simeq -180^o$] is reduced by the direct radial field of the feedback coil. No such reduction takes place for the poloidal sensors. This exemplifies a rather general rule, that direct effects of the actuator system on the sensor degrade control.

Figure 3 shows how the "critical gain" $|K_{\rm cr}|$ (i.e., minimum $|K|$ for complete stabilization) depends on the poloidal width of the active coil, assuming current control $\tau = 0$. The gain K is defined as the ratio of the opposing *radial* field, at the sensor position, *generated by the active coil*, to the *total* field measured by the sensor (whatever the orientation of the sensor). Figure 3 compares b_r-sensor feedback (dashed lines) using sensors rather close to the plasma ($r_f = 1.225a, r_s^r = 1.05a$) and b_θ-sensor feedback (solid lines) with all the coils further away

($r_f = 1.3a, r_s^\theta = 1.1875a$). The critical proportional gain for $\arg(K) = 0^o$ and 30^o and both types of sensor is shown.

For both schemes, the optimal α, that minimizes the critical gain, is about 0.55, but poloidal sensors give a much larger range of coil widths where the stabilization is possible. The b_r-sensor also requires higher gain than a b_θ-sensor. We conclude that a b_θ-sensor is vastly superior to a b_r-sensor for RWM stabilization.

3. Controller design

For the design of robust controllers, we considered a set of equilibria with ITER-FEAT geometry, with parameters given in Table 1. The no-wall limit of β_N is 2.55 for $q_{\min} = 3.5$, and 2.39 for $q_{\min} = 2.2$.

EQ	$q_{\min}$	β_N	I_N	$f_{\rm bs}$
1	3.5	3.05	1.33	0.87
2	3.5	3.71	1.39	1.00
3	2.2	3.90	2.03	0.74
4	2.2	4.95	2.11	0.90

Table 1: Four ITER-FEAT equilibria.

We studied two types of feedback coil winding, broad strips and thin wires, which give different self-inductance $P_2(s)$. In the case of broad strips, $P_2(s)$ is computed numerically. In the thin-wire limit, $P_2(s)$ is dominated by the frequency independent contribution from the near field, therefore, $P_2(s) \equiv 1$. The corresponding process transfer functions (1) are denoted by $G_1(s)$ and $G_2(s)$, for broad strips and thin wires, respectively.

The goal of the control design is to find a controller $K(s)$, such that the system, with the closed loop transfer function $L(s) = K(s)G(s)$ satisfies certain performance criteria for all the equilibria. The first performance criterion is the stability margin $J_S = \max_\omega |1/[1 + L(j\omega)]|$, which must be small enough. The second stability margin $J_T = \max_\omega |L(j\omega)/[1 + L(j\omega)]|$ restricts the overshoot of the system time response. Default values often used are $J_S = 1.7$, and $J_T = 1.3$. The "control activity" connected with measurement noise is quantified by $J_u = \max_\omega |K(j\omega)/[1 + L(j\omega)]|$. A low-frequency measure $J_{LF} = 1/K(0)$ is defined to measure the load disturbance compensation.

We designed controllers by minimizing J_{LF}, with the constraints $J_S \leq 2.0$, $J_T \leq 2.5$ and $J_u \leq 8$. Robustness was achieved by considering all the four equilibria in Table 1. The optimization was performed for various τ values, and the maximum τ values achieved are shown in Tables 2 and 3.

Several types of controllers were considered, including proportional $K_p(s) = k_p$, PD controllers with additional derivative action $K_{PD}(s) = k_p(1 + T_d s)/(1 + sT_d/\eta)$ and $\mathcal{H}_\infty$ controllers. There are a few different approaches to obtain an optimal $\mathcal{H}_\infty$ controller, and we implemented the so-called $\mathcal{H}_\infty$ loop shaping design technique [8], with a weight function $W(s)$. The weight function $W(s)$ can be chosen to be K_P or K_{PD}, we then obtain $\mathcal{H}_{\infty P}$ or $\mathcal{H}_{\infty PD}$ controller. This type of controllers will, in some sense, have optimal robustness (stability margins).

Ctrl.	J_u	J_{LF}	τ	T_d	η
K_P	2.8	0.71	0.5		
K_{PD}	8.0	0.41	2.6	0.29	2.6
$\mathcal{H}_{\infty P}$	8.0	0.96	3.5		
$\mathcal{H}_{\infty PD}$	8.0	1.30	4.0	3.6	6.8

Table 2: Results for equilibrium 4 and G_1 (broad strips).

Ctrl.	J_u	J_{LF}	τ	T_d	η
K_P	1.8	1.1	0.09		
K_{PD}	8.0	1.2	0.96	0.75	9.5
$\mathcal{H}_{\infty P}$	8.0	1.0	0.85		
$\mathcal{H}_{\infty PD}$	8.0	1.3	0.94	0.99	2.0

Table 3: Results for equilibrium 4 and G_2 (thin wires).

From the tables we note that broad conductors (G_1) can handle about 3 times longer response time than thin wires (G_2). This,

plus the lower inductive voltage produced by broad strips, makes them clearly superior to thin wires for RWM control. Next, the trade off between τ and the degree of freedom in the P and PD controllers can be noted. By using three tuning parameters, instead of one, τ can be increased significantly. The PD controller reaches τ within 20-30% of the $\mathcal{H}_\infty$ controllers.

As might be expected, the limitation in τ comes from the fourth equilibrium with the highest pressure (more than twice the no-wall limit). An important conclusion is that a controller that works at a certain pressure is well behaved also at lower pressure, with the same τ value. Therefore, controllers do not have to be modified dynamically. Somewhat surprisingly, the controller optimized for the fourth equilibrium cannot handle longer response times for the other equilibria with lower pressure.

However, if we disregard the high-pressure equilibrium, the controller may be reoptimized for longer response times. We optimized controllers for the third equilibrium, which exceeds the no-wall beta limit by 63%. For the three first equilibria, the optimal PD controller satisfies the performance criteria for τ up to 5.4 (broad strips) and 2.1 (thin wires). For the $\mathcal{H}_{\infty PD}$ controller, the limits to τ are 10.3 and 2.4, respectively.

4. Summary

We have formulated and studied the control problem for non-axisymmetric resistive wall modes in tokamaks. The open-loop transfer function for the plasma-wall system is constructed from toroidal stability calculations. Poloidal sensors were found to be clearly better than radial sensors. With poloidal sensors placed just inside the wall and feedback coils outside, robust RWM control can be implemented and work well, for reasonable time constants, even far above the no-wall beta limit. In the future, we plan to analyze tokamaks with double walls, as proposed for ITER-FEAT, to see under what circumstances a feedback system with the sensors between the two walls will work.

Acknowledgment. We thank Dr Tony Taylor (General Atomics) for suggesting the use of poloidal sensor coils.

References

[1] F. Troyon, et al, Plasma Phys. Controll. Fusion **26**, 209 (1984).

[2] T. S. Taylor, et al, Proc. 13th IAEA Conf. Washington DC 1990, vol. 1, p. 177.

[3] M. Okabayashi, *et al.*, Proceedings of the 26th EPS Conference on Controlled Fusion and Plasma Physics, Maastricht, the Netherlands, 1999, Vol. 23J, p. 1661 (European Physical Society, Petit-Lancy, 1999).

[4] M. Okabayashi, N. Pomphrey, and R. E. Hatcher, Nucl. Fusion **38**, 1607 (1998).

[5] Y. Q. Liu and A. Bondeson, Phys. Rev. Lett. **84**, 907 (2000).

[6] Y. Q. Liu, et al, "Feedback stabilization of non-axisymmetric resistive wall modes in tokamaks. Part 1: Electromagnetic model", Phys. Plasmas, accepted (2000).

[7] C. M. Fransson, et al, "Feedback stabilization of non-axisymmetric resistive wall modes in tokamaks. Part 2: Control analysis", Phys. Plasmas, submitted (2000).

[8] D. MacFarlane and K. Glover, IEEE Trans. Autom. Contr., **37**, pp. 759-769 (1992).